

2.3 Spatial pattern of the heat budget components

The mean latitudinal values of the heat budget components discussed above conceal great spatial variations. Figure 2.4 shows the global distribution of the annual net radiation at the surface. Broadly, its magnitude decreases poleward from about 25° latitude. However, as a result of the high absorption of solar radiation by the sea, net radiation is greater over the oceans – exceeding 160 W m^{-2} in latitudes 15–20° – than over land areas, where it is about $80\text{--}105\text{ W m}^{-2}$ in the same latitudes.

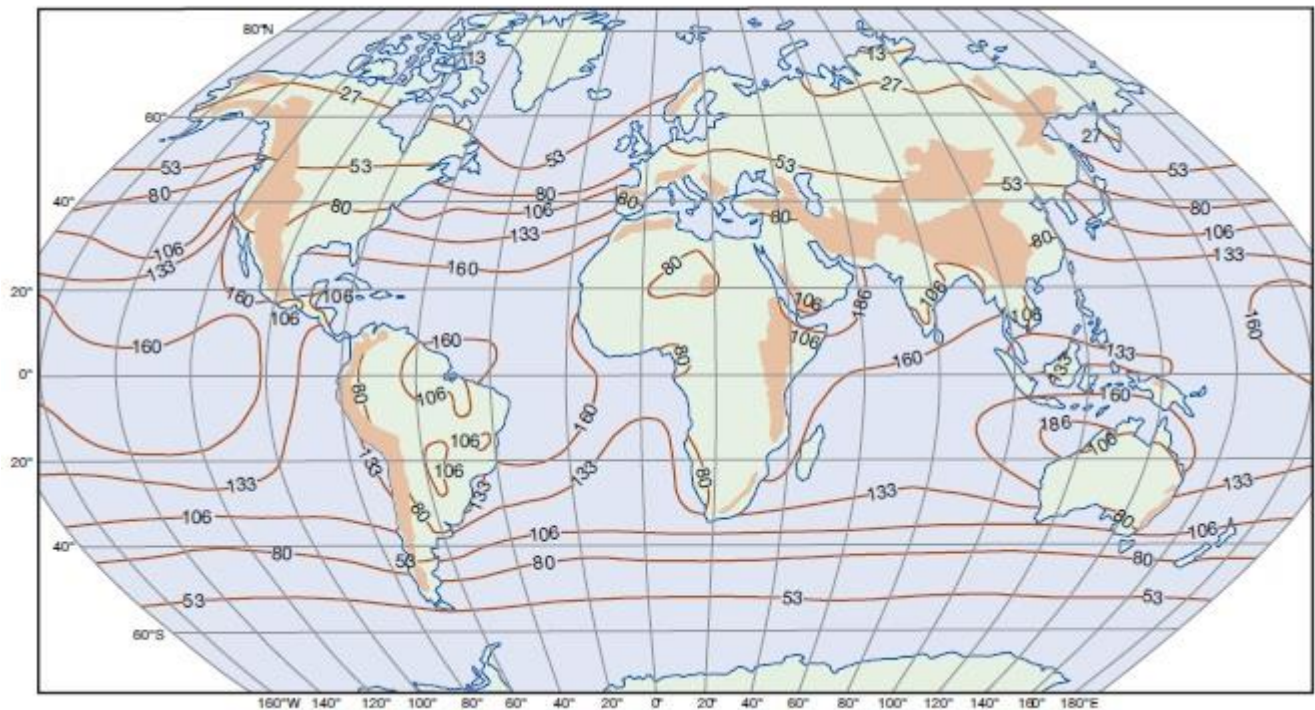


Figure 2.4: Global distribution of the annual net radiation at the surface, in W m^{-2} .

Net radiation is also lower in arid continental areas than in humid areas, because in spite of the increased insolation receipts under clear skies there is at the same time greater net loss of terrestrial radiation. Figures 2.5 and 2.6 show the annual vertical transfers of latent and sensible heat to the atmosphere. Both fluxes are distributed very differently over land and seas. Heat expenditure for evaporation is at a maximum in tropical and subtropical ocean areas, where it exceeds 160 W m^{-2} . It is

less near the equator, where wind speeds are somewhat lower and the air has a vapor pressure close to the saturation value. It is clear from Figure 2.5 that the major warm currents greatly increase the evaporation rate. On land, the latent heat transfer is largest in hot, humid regions. It is least in arid areas with low precipitation and in high latitudes, where there is little available energy or moisture. The largest exchange of sensible heat occurs over tropical deserts, where more than 80 W m^{-2} is transferred to the atmosphere (see Figure 2.6). In contrast to latent heat, the sensible heat flux is generally small over the oceans, only reaching $25\text{--}40\text{ W m}^{-2}$ in areas of warm currents. Indeed, negative values occur (transfer to the ocean) where warm continental air masses move offshore over cold currents.

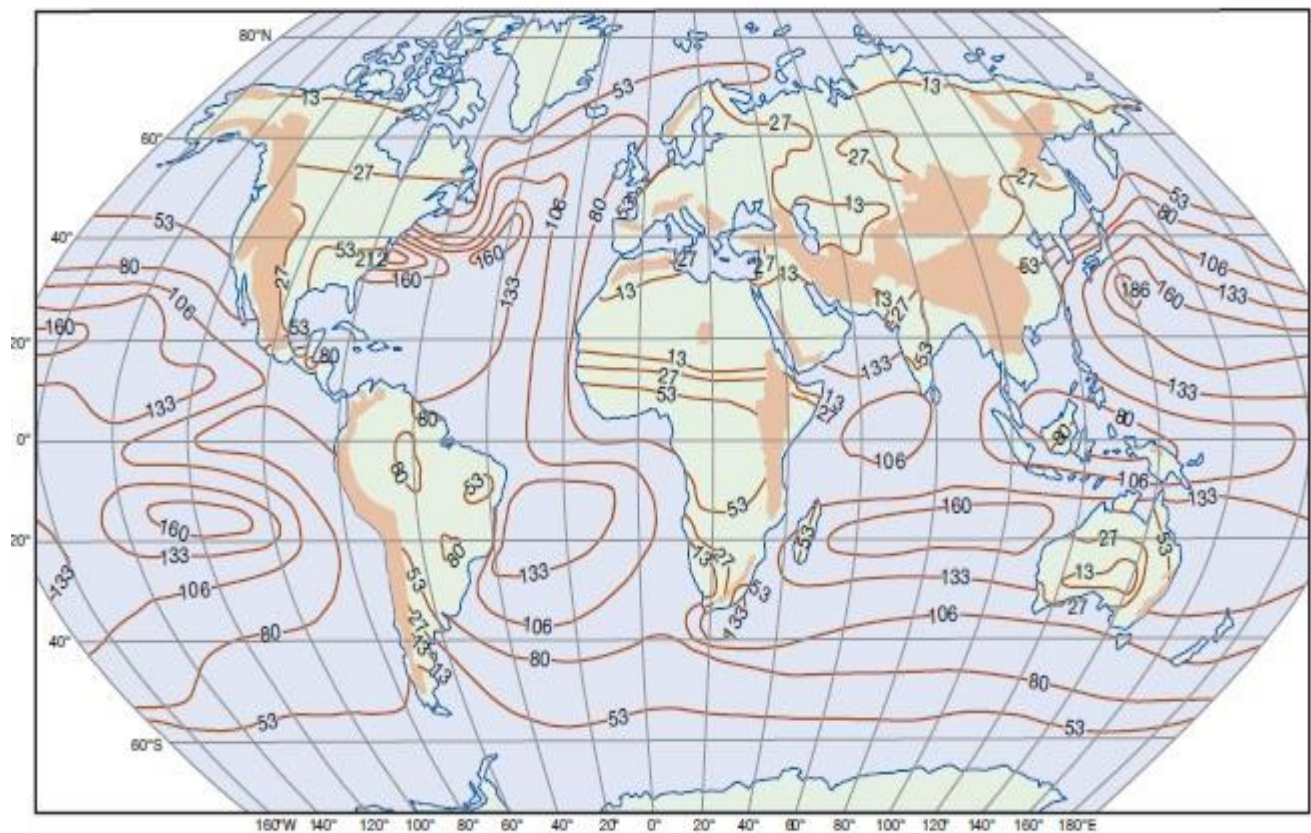


Figure 2.5: Global distribution of the vertical transfer of latent heat, in W m^{-2} .

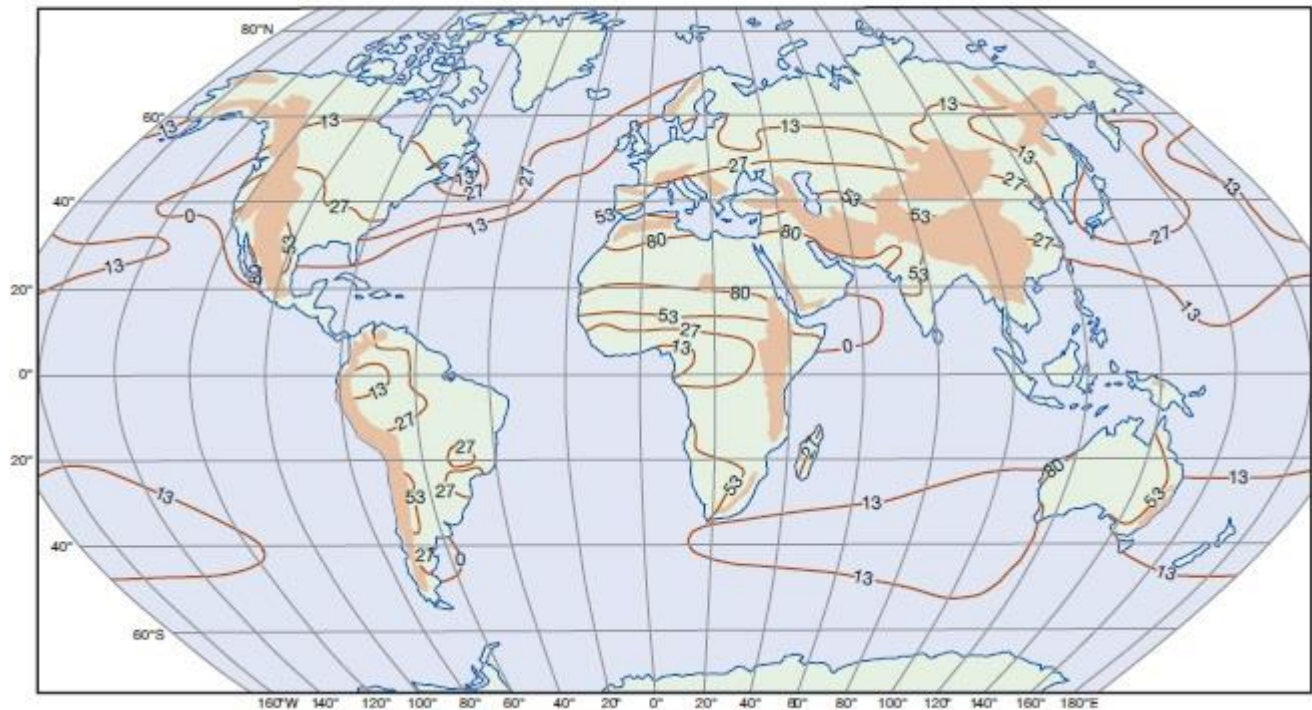


Figure 2.6: Global distribution of the vertical transfer of sensible heat, in W m^{-2} .

2.4 The greenhouse effect

The natural greenhouse effect of the earth's atmosphere is attributable primarily to water vapor. It accounts for 21K of the 33K difference between the effective temperature of a dry atmosphere and the real atmosphere through the trapping of infrared radiation. Water vapor is strongly absorptive around $2.4\text{--}3.1\mu\text{m}$, $4.5\text{--}6.5\mu\text{m}$ and above $16\mu\text{m}$. The concept of greenhouse gas-induced warming is commonly applied to the effects of the increases in atmospheric carbon dioxide concentrations resulting from anthropogenic activities, principally the burning of fossil fuels. Sverre Arrhenius in Sweden drew attention to this possibility in 1896, but observational evidence was only forthcoming some 40 years later (Callendar, 1938, 1961). However, a careful record of atmospheric concentrations of carbon dioxide was lacking until Charles Keeling installed calibrated instruments at the Mauna Loa

Observatory, Hawaii, in 1957. Within a decade, these observations became the global benchmark.

They showed an annual cycle of about 5ppm at the Observatory, caused by the biospheric uptake and release, and the ca. 0.4 percent annual increase in CO₂, from 315ppm in 1957 to 383ppm in 2007, due to fossil fuel burning. The annual increase is about half of the total emission due to CO₂ uptake by the oceans and the land biosphere. The principal absorption band for radiation by carbon dioxide is around 14–16μm, but there are others at 2.6 and 4.2μm. Most of the effect of increasing CO₂ concentration is by enhanced absorption in the latter, as the main band is almost saturated. The sensitivity of mean global air temperature to a doubling of CO₂ is in the range 2–5°C, while a removal of all atmospheric CO₂ might lower the mean surface temperature by more than 10°C.

The important role of other trace greenhouse gases (methane, nitrous oxide, fluorocarbons) was recognized in the 1980s and many additional trace gases began to be monitored. The latest is nitrogen trifluoride used during the manufacture of liquid crystal flat-panel displays, thin-film solar cells and microcircuits. Although concentrations of the gas are currently only 0.454 parts per trillion, it is 17,000 times more potent as a global warming agent than a similar mass of carbon dioxide. The past histories of greenhouse gases, reconstructed from ice core records, show that the preindustrial level of CO₂ was 280ppm and methane 750ppb compared with 383ppm and 1790ppb, respectively, today. Their concentrations decreased to about 180 ppm and 350ppb, respectively, during the maximum phases of continental glaciation in the Pleistocene Ice Age. The positive feedback effect of CO₂, which involves greenhouse gas-induced warming leading to an enhanced hydrological cycle with a larger atmospheric vapor content and therefore further warming, is still not well resolved quantitatively.